Published in final edited form as:
*Biomaterials*. 2012 November ; 33(32): 7933–7944. doi:10.1016/j.biomaterials.2012.07.027.

# Diazeniumdiolate-Doped Poly(lactic-*co*-glycolic acid)-Based Nitric Oxide Releasing Films as Antibiofilm Coatings

**Wenyi Cai**[1], **Jianfeng Wu**[2], **Chuanwu Xi**[2,*], and **Mark, E. Meyerhoff**[1,*]

[1]Department of Chemistry, The University of Michigan, Ann Arbor, MI, 48109, USA

[2]Department of Environmental Health Sciences, The University of Michigan, Ann Arbor, MI, 48109, USA

## Abstract

Nitric oxide (NO) releasing films with a bilayer configuration are fabricated by doping dibutyhexyldiamine diazeniumdiolate (DBHD/$N_2O_2$) in a poly(lactic-*co*-glycolic acid) (PLGA) layer and further encapsulating this base layer with a silicone rubber top coating. By incorporating pH sensitive dyes within the films, pH changes in the PLGA layer are visualized and correlated with the NO release profiles (flux vs. time). It is demonstrated that PLGA acts as both a promoter and controller of NO release from the coating by providing protons through its intrinsic acid residues (both end-groups and monomeric acid impurities) and hydrolysis products (lactic acid and glycolic acid). Control of the pH changes within the PLGA layer can be achieved by adjusting the ratio of DBHD/$N_2O_2$ and utilizing PLGAs with different hydrolysis rates. Coatings with a variety of NO release profiles are prepared with lifetimes of up to 15 d at room temperature (23 °C) and 10 d at 37 °C. When incubated in a CDC flow bioreactor for a one-week period at RT or 37 °C, all the NO releasing films exhibit considerable antibiofilm properties against gram-positive *S. aureus* and gram-negative *E. coli*. In particular, compared to the silicone rubber surface alone, an NO releasing film with a base layer of 30 wt% DBHD/$N_2O_2$ mixed with poly(lactic acid) exhibits an ~98.4% reduction in biofilm biomass of *S. aureus* and ~ 99.9% reduction for *E. coli* at 37 °C. The new diazeniumdiolate-doped PLGA-based NO releasing coatings are expected to be useful antibiofilm coatings for a variety of indwelling biomedical devices (e.g., catheters).

### Keywords

Biofilm; Nitric oxide; Diazeniumdiolate; Poly(lactic-*co*-glycolic acid)

## 1. Introduction

Biofilm-based bacterial infection is a common problem for indwelling biomedical devices and artificial prosthetics [1]. Acting via a “cooperative community” [2], a biofilm will irreversibly colonize the surface while protecting the microorganisms inside a matrix of extracellular polymeric substances (EPSs). Due to this protection, a significantly increased



Corresponding authors: Mark E. Meyerhoff Department of Chemistry, The University of Michigan 930 N University, Ann Arbor, MI, 48109; Chuanwu Xi Department of Environmental Health Sciences, The University of Michigan 1415 Washington Hts Ann Arbor, MI 48109. *Telephone: +1-734-763-5916 mmeyerho@umich.edu; Telephone: +1-734-615-9594 cxi@umich.edu.

dosage of antibiotics or device removal will normally be necessary to treat biofilm derived infections [1, 3].

To reduce medical costs and decrease risk of serious infection, various strategies have been used to develop antimicrobial/antibiofilm coatings for indwelling devices. While numerous strategies including the application of hydrophilic polysaccharides, poly(ethylene glycol), surfactants, positively charged polymer brushes or proteins have been applied to modify the device surface [4, 5], the effectiveness of these type of non-releasing coatings, however, varies with bacterial species [1, 6] and might be weakened through formation of conditioning films. An alternative strategy is to use coatings that can release antimicrobial agents. However, the resistance of an increasing number of bacterial strains and biofilms to antibiotics has limited the practical application of most antibiotic-releasing coatings [3]. Recently, silver salts [7] or silver nanoparticle-based coatings [8] have been shown to prevent bacterial adhesion and biofilm formation on surfaces, but the cytotoxicity and genotoxicity of silver ions remain a potential issue [5].

Nitric oxide (NO), an endogenous bactericidal agent that is produced in large quantities by macrophages exhibits antimicrobial properties against a broad spectrum of bacteria. It is reported that NO is able to kill bacterial cells by direct or indirect oxidation mainly through formation of peroxynitrite ($^{-}$OONO), the product of the reaction of NO with superoxide ($O_2^{\bullet -}$). Nitric Oxide is also able to nitrosate cysteine and tyrosine residues which will lead to dysfunction of bacterial proteins [1]. In addition, a significantly low level of NO is reported to prevent biofilm formation and disperse established biofilm through a signaling process [2, 9-11]. Although the antimicrobial and antibiofilm properties of NO releasing coatings have been studied, most *in vitro* studies have been performed under “static” conditions [12], which is not normally correlated with the natural life cycle of bacteria [13]. Recently, the Schoenfisch group has used a parallel plate flow cell that creates shear forces to mimic the natural environment encountered by microbes, and studied the decrease in microbial attachment on NO release coatings after 2 h in PBS buffer [12, 14]. Compared to this and other previous reported systems, a flow-through CDC (Centers for Disease Control and Prevention) biofilm reactor, capable of creating both renewable nutrient sources and shear forces, is regarded as a standard tool to study biofilm formation under natural conditions for longer time periods with repeatable results [13].

As the most studied class of NO donors, diazeniumdiolates have been utilized to prepare NO release polymer coatings that prevent thrombus formation [15] and reduce bacterial adhesion [1]. The applications of these NO donors, however, are limited due to potential toxicity issues derived from the leaching of diazeniumdiolates and product amines from the NO releasing coatings. Although diazeniumdiolates can be covalently attached onto the polymeric backbone to reduce the toxicity, a facile way is to dope lipophilic diazeniumdiolates into a polymer film [15] and then further coat this layer with a top coat of polymer that decreases the leaching of the diazeniumdiolate or product amine, but allows rapid diffusion of NO out of the bilayer film. Previously, our group has demonstrated that dibutyhexyldiamine diazeniumdiolate (DBHD/$N_2O_2$) (Fig. 1) can be used as a stable lipophilic NO donor in polymeric membranes to release NO with minimal leaching [16]. Due to the proton-driven NO release mechanism of diazeniumdiolates, the challenge of utilizing a DBHD/$N_2O_2$ doped coating lies in controlling the NO release profile and extending its lifetime by controlling the pH within the polymeric material. Recently, poly (lactic-*co*-glycolic acid) (PLGA) (Fig. 1), a biodegradable and biocompatible polymer that is approved by the U.S. Food and Drug Administration (FDA), was employed as a matrix to promote the NO release of DBHD/$N_2O_2$ incorporated as a coating (with outer coating of polyurethane) within an NO releasing intravascular glucose sensor that exhibited greatly reduced thrombus formation [17]. However, no previous study has been conducted to

correlate the change in pH within the PLGA-based bilayer film with the NO release profile, resulting in an unclear mechanism for PLGA as an NO release promoter. Further, such coatings have never been examined with respect to antimicrobial/antibiofilm behavior.

Herein, we describe a two-layered NO release coating with a base layer of DBHD/$N_2O_2$ doped in PLGA and a protective silicone rubber (SR) top coating (see Fig. 2 for film configuration). The pH changes in the PLGA layer are visualized by incorporating a pH sensitive dye into the coating. By employing PLGAs with different hydrolysis rates as the inner matrix (possessing different ratios of lactic and glycolic acid in the PLGA polymer), the NO release profile of this type of coating can be readily manipulated, which in turn, greatly impacts the NO release kinetics. The antibiofilm properties of these new NO releasing coatings against gram-positive *S. aureus* and gram-negative *E. coli* at room temperature (23 °C) and physiological temperature (37°C) are evaluated after a one week incubation in a CDC biofilm flow-reactor.

## 2. Materials and Methods

### 2.1 Materials

Acid terminated poly(D, L-lactide-*co*-glycolide acid) (PLGA) 50:50 (a-50-50) (catalog number 719897) was purchased from Sigma-Aldrich (St. Louis, MO) and ester terminated PLGA e-50-50, e-75-25, e-PLL (with catalog numbers of 5050 DLG 7E, 7525 DLG 7E and 100 DL 7E, respectively) were purchased from SurModics Pharmaceuticals (Birmingham, AL). Silicone rubber RTV 3140 was obtained from Dow Corning Corporation (Midland, MI). Tecoflex polyurethane SG-80A was a gift from Lubrizol Advanced Materials (Cleveland, OH). Bromocresol purple was obtained from Fisher Scientific (Pittsburg, PA) and bromothymol blue was obtained from Sigma-Aldrich (St. Louis, MO). Phosphate buffered saline (PBS), pH 7.4, containing 137 mM NaCl, 2.7 mM KCl, 10 mM sodium phosphate, was used in all experiments. Tetrahydrofuran (THF) was obtained from Fisher Scientific (Pittsburgh, PA) and was distilled over sodium and benzophenone prior to use. All aqueous solutions were prepared with deionized water from a Milli-Q system (18 MΩ $cm^{-1}$; Millipore Corp., Billerica, MA). *Escherichia coli* K-12 MG16653 and *Staphylococcus aureus* ATCC 45330 were purchased from American Type Culture Collection. Luria Bertani (LB) agar and broth were products of Fisher Scientific Inc. (Pittsburgh, PA).

DBHD/$N_2O_2$ was synthesized by treating N, N'-dibutyl-1, 6-hexanediamine (DBHD, Aldrich) with NO gas (80 psi, Cryogenic Gases (Detroit, MI)) at RT for three days as previously described [16]. DBHD/$N_2O_2$ and PLGA were stored in a desiccator at -20 °C before use.

### 2.2 Preparation of NO releasing films

Glass slides (0.9 × 5 cm) were cleaned by sonicating in acetone, deionized water and acetone sequentially and dried before use. Two hundred mg of given type of PLGA was dissolved in 3 mL THF and 50 mg or 86 mg DBHD/$N_2O_2$ was then added to the solution to form a cocktail containing 20 wt% or 30 wt% of the NO donor, respectively. The cocktail was then sonicated until a homogeneous dispersion was formed. Twenty five microliters of the dispersion was then cast in an O-ring on a glass slide to form an NO-releasing base layer. The O-ring was then removed and the remaining layer was allowed to dry. This procedure was repeated another three times. Then, 100 μL of SR solution (160 mg $mL^{-1}$ in THF) was then casted over the NO-release PLGA layer as a top coating. The NO releasing layer was fully covered by the top coating (see Fig. 2). The bilayer film was then dried in air for one day and in vacuum with desiccants for two days to remove residual solvent before testing. The diameter of the NO releasing layer was 7 mm. All the controls were prepared in

the same way as the NO releasing films, except PLGA alone or PLGA mixed with DBHD was used as the base layer. In addition, for comparison, silicone rubber and polyurethane were also used to replace PLGA as matrices for the underlying layer. The thickness of the PLGA-based NO releasing layer as determined by Scanning Electron Microscope (SEM) was 100~130 μm and the thickness of the SR top coating was 120 μm (see Fig. 1S in Supporting Information). SEM images were taken on an Amray FE 1900 Scanning Electron Microscope (SEM) at a working distance of 12 mm at 5 kV. The films were sputter-coated with gold for 30 s before imaging. The thickness of the top coating was optimized by evaluating the leaching of DBHD from films containing a base layer of 20 wt % DBHD mixed with a-50-50 PLGA with different top coating thicknesses using a Micromass LCT Time-of-Flight mass spectrometer. The MS spectra comparison and experimental details are listed in Supporting Information, Fig. 2S.

### 2.3 Evaluation of solution pH and pH changes in films

Ten microliters of 5 mM solutions of the pH probes (in THF) were added into 300 μL PBS buffers with pHs ranging from 3 to 8, respectively, in a round bottom 96-well microplate, and the image of the twelve wells was recorded to obtain the color chart of the two indicators. Dispersions were then prepared as indicated in Section 2.2 and the indicator solutions were added to the NO release or control PLGA dispersions to reach a final concentration of 10 mmol $kg^{-1}$ [18]. The colors of the dispersions were compared rightly after the dispersions were prepared. For in-situ pH assessment, the films were stored in pH 7.4 PBS in uncapped scintillation vials at R.T. (23 °C) or 37 °C. The solutions were replaced daily and the images of the films in PBS buffer were taken at different time points.

### 2.4 NO release measurements

The NO release profiles of the bilayer coatings were measured by purging $N_2$ into 2 mL PBS buffer solution, pH 7.4, in a glass cell protected from light and monitored using a chemiluminescence NO analyzer (NOA) (Sievers 280, Boulder, CO). The NOA calibration curve was obtained by adding nitrite to an acidified potassium iodide solution and plotting the integrated signal (ppb ×s) vs. moles of NO that were introduced into the system [19]. The films were stored as described in Section 2.3, the NO production was measured by NOA and the NO fluxes at different time points were calculated using the calibration curve. The flux values were reported as average ± standard deviation calculated from the fluxes of two films with the same formulation.

### 2.5 *In vitro* antimicrobial test

Overnight LB (Luria Bertani) broth grown bacterial cultures were washed with 1×PBS buffer three times, and resuspended in 1×PBS buffer to make a final cell concentration at ~$10^8$ CFU/mL. Each NO releasing or control film was placed into a Corning 15-mL tube with 2 mL of the washed bacterial culture solution. The tube was incubated at 37 °C for 2 h or 24 h while horizontally shaking at 150 rpm. After incubation, the films were removed aseptically and the bacterial culture was serially diluted 10-fold in 1×PBS buffer and 50 μL of each dilution was plated onto an LB agar plate for viable bacterial counting. All the experiments were conducted in duplicate.

### 2.6 *In vitro* antibiofilm testing

A CDC flow bioreactor (Biosurface Technologies, Bozeman, MT) was used for the antibiofilm testing. The CDC bioreactor with its coupon holders was autoclaved before use. Coated slides were mounted on the coupon holders and the reactor was supplemented with 10% LB medium by a peristaltic pump with a continuous flow rate of 100 ml/h. Overnight bacterial cultures were 1:100 diluted and inoculated into the glass vessel of CDC reactor

aseptically. The liquid growth medium was circulated through the vessel and shear force was generated by a magnetic stir bar rotated by a magnetic stir plate. Biofilms developed on the surface of coated slides were completely immersed into the circulating culture. The CDC bioreactor was set up on the bench at room temperature (23 °C) or in an incubator at 37 °C.

After a 7 d incubation, coated slides were aseptically removed and individual slides were transferred to a petri dish for further staining with LIVE/DEAD® BacLight™ Bacterial Viability kit (L7012, Invitrogen, Carlsbad, CA) according to instructions in the reagent manual. Fluorescent images were acquired with a fluorescence microscope (Olympus 1×71, Center Valley, PA) equipped with Fluorescence Illumination System (X-Cite 120, EXFO) and filters for SYTO-9 (ex. 488 nm/em. 520 nm) and Propidium Iodide (ex. 535 nm/em. 617 nm) fluorescence. Images were obtained using an oil immersion 60 × objective lens. The slides were also examined under an Olympus FluoviewTM FV1000 confocal microscope (Olympus, Markham. Ontario) with Melles Griot Laser supply, detectors and appropriate filter sets. Three different spots on the NO releasing area of each film were randomly chosen for obtaining both 2D and 3D images. Simulated 3D images were reconstructed using the Amira software package (Amira, San Diego, CA) and biofilms biomass values were quantified using the COMSTAT software (version 1) [20] with the threshold setting as 25.

## 3. Results and Discussion

### 3.1 Selecting pH-sensitive probes for assessing film pH profiles

It has been reported that at a given temperature, the decomposition of intramolecular zwitterionic diazeniumdiolates such as DBHD/$N_2O_2$ is proton dependent [21]. The NO release rate decreases as the environmental pH increases [16]. Therefore, to understand and control the release profile of DBHD/$N_2O_2$-based NO releasing coatings, it is important to monitor the film pH changes as a function of time.

Previously, it was shown that the pH change of a DBHD/$N_2O_2$-based NO releasing PVC coating could be evaluated by incorporating a lipophilic pH chromoionophore in the film and comparing the UV-Vis spectra of the film at different time points [16]. This method, however, suffers from the interference from light scattering due to the insolubility of DBHD/$N_2O_2$ in such polymer films. Recently, the Schwendeman group developed a confocal fluorescence microscope imaging method to directly quantify the microclimate pH distribution in PLGA microspheres using a pH-sensitive probe [22]. As alternatives to fluorescence probes, common pH indicators offer a facile, inexpensive and a more convenient means to semi-quantitatively visualize the pH changes within polymer films [23].

To effectively evaluate the pH change in the NO releasing coatings during a prolonged time period, the pH probe needs to be sensitive enough to change color during the NO release and PLGA hydrolysis processes. As shown in Fig. 2B, within an NO releasing film, DBHD/$N_2O_2$ releases NO through a proton driven mechanism and produces the diamine DBHD, that will further react with water to increase the pH within the polymer phase. In contrast, the hydrolysis of PLGA that takes place simultaneously will produce lactic and glycolic acids that will decrease the pH in the film. Therefore, the indicator must change color in a pH range that will allow visualization of the acidic or basic environment created by the reactions within the PLGA layer.

Based on the above requirements, two sulfonephthaleins, bromocresol purple (BP) and bromothymol blue (BB), were selected as the pH-sensitive probes [14] and added into the PLGA dispersions employed in this work. As shown from the color chart in Fig. 3, in PBS buffers with pH values ranging from 3-8, the color of bromocresol purple (BP) changes from

yellow to purple with a transition pH range of 5-6. For bromothymol blue (BB), the color changes from yellow to green and blue at a higher transition pH range of 6-8. The indicators were then added into different solutions or dispersions of the a-50-50 PLGA and DBHD or DBHD/$N_2O_2$ and the colors were compared (see Fig. 3). A THF solution containing 20 wt% of the DBHD diamine was used to represent an extreme case, in which all the NO was released from the NO donor DBHD/$N_2O_2$ while neglecting the hydrolysis of PLGA. In the real situation, the film pH would be lower because the hydrolysis of PLGA will produce small molecular acids to neutralize the base. Therefore, a good probe should at least be able to distinguish the difference between a mixture containing 20 wt% of the NO donor DBHD/$N_2O_2$ in a-50-50 PLGA and a solution of 20 wt% DBHD in a-50-50 PLGA. As shown in Fig. 3, for each of the indicators, a distinguishable color difference between the two mixtures is observed, indicating a much more basic pH environment once the NO is totally released leaving the free diamine species. (note: such pH differences were further confirmed for given THF solutions using a glass pH electrode (Corning pH meter 240, Accumet 13-620-286) to determine the pH. For example, a 20 wt% DBHD in a-50-50 PLGA solution prepared in THF has a measured pH value of 9.2, while the PLGA alone in THF exhibits a measured pH value of 5.1). In addition, for both indicators, a suspension of DBHD/$N_2O_2$ exhibits a transition color totally different from the above two mixtures, indicating the sensitivity of both pH probes. It is also clear from the color difference that a-50-50 PLGA alone is the most acidic solution [22]. Meanwhile, it is difficult to differentiate the acidity within the PLGA and SR solutions due to the narrow transition pH range of both pH probes. However, this does not affect their capability to be used to indicate film pH changes of the NO releasing coatings when the DBHD/$N_2O_2$ species is present.

### 3.2 Correlating film pH with NO release profile

The release of NO from DBHD/$N_2O_2$ will produce DBHD and further raise the film pH and decrease the NO release rate for diazeniumdiolates [16]. Without any additives such as tetraphenylborate or PLGA to adjust the pH in the active layer of the coating, the NO flux of the NO releasing coating is low and its lifetime is short [16, 17]. More recently, our group demonstrated that PLGA can be used as a non-toxic matrix under a polyurethane top coating to promote the NO release of DBHD/$N_2O_2$ in a two-layered NO releasing coating employed to prepare implantable glucose and lactate catheters [17].

For the present study, the DBHD/$N_2O_2$ was first doped directly into PLGAs that possess different hydrolysis rates to prepare different base layers [24]. As shown in Fig. 2A, the coatings used have a bilayer configuration with the inner layer comprised of DBHD/$N_2O_2$ embedded in the PLGA matrix. The outer layer is a SR top coating, which is used to protect the inner layer, extend the NO release period and prevent leaching of species (e.g., DBHD products, etc.) from the membrane into the surrounding solution. The bilayer structure is schematically illustrated in Fig. 2B.

PLGA has been widely used in biomedical applications (e.g., drug delivery) not only due to its biocompatibility, but also because of the controlled degradation that can be achieved by controlling the end groups as well as the lactide to glycolide ratio within the polymeric chain [24]. Therefore, we wanted to examine the NO release profiles of films containing PLGA possessing different hydrolysis rates at different temperatures. Toward this end, the NO release profiles and film pH changes of two NO releasing coatings prepared with 20 wt% DBHD/$N_2O_2$ incorporated into two different types of PLGA matrices at RT (23 °C) were initially studied. Both PLGAs had a lactide to glycolide ratio of 50:50, but the end groups were acids and esters, respectively. The NO release profiles of the films were monitored daily until the depletion of the NO donor and the results are shown in Fig. 4A. The film with the acid-capped PLGA (a-50-50) exhibits a gradual decreasing NO flux over time, while there is no significant variation in the daily NO flux of the bilayer film prepared with the

ester-capped PLGA (e-50-50) after the second day of the NO release period. Further, although the daily NO flux of the e-50-50-based film is lower compared to the film prepared with the a-50-50 material, the NO release lifetime is extended from 10 d to a 15 d period.

To further explain the NO release patterns observed, the two pH sensitive probes were further incorporated into the polymeric films to evaluate the pH changes over time. As shown in Fig. 5A, as soon as the films are in contact with solution, both probes indicate a more basic environment for the e-50-50-based film due to the difference in end groups (ester capped; i.e., little or no free acidic groups present). Within 3 h of NO release, an increase of film pH is already observed for both films and this basicity becomes more obvious after a 24 h period. After the second day, however, due to the continued and faster hydrolysis of the a-50-50 PLGA, a gradual decrease in the film pH begins to be observed for the a-50-50-based film (Fig. 5A-a and Fig. 5A-c). The e-50-50, on the other hand, degrades much more slowly, resulting in a much less obvious color change of the pH probe incorporated into this layer (Fig. 5A-b and Fig. 5A-d). It should be noted that during the preparation of the multilayer films, the active layers were cast using an O-ring. Since the diazeniumdiolate species is insoluble, it will mainly be in the central area (does not spread out as much) while there is more PLGA in the peripheral cap region and this causes the difference in color (pH values) between the very center regions and the edges in Fig. 5 images.

Based on the above observations, a mechanism is proposed to further explain the difference in release profiles for the two NO releasing coatings. As shown in Fig. 2B, as soon as the NO releasing coating is in contact with solution, when water penetrates the SR outer layer and contacts the PLGA matrix, the carboxyl end groups and hydrolysis products of residue monomers present in the matrix will provide a proton source to enhance the release of NO from the donor through a proton-driven mechanism. At a given temperature, the NO flux is highly dependent on the pH within the film, which is further dependent on the end group type and monomer residue ratio of the PLGA matrix. Therefore, the a-50-50 shows a much higher NO starting flux compared to the e-50-50 material with the same ratio of monomer residues (see Supporting Information Table 1S) to promote the initial NO release. Once NO is released, the diamine DBHD will remain in the film and form ammonium salts of hydroxide and this process will further facilitate the hydrolysis of PLGA to produce more protons and thus promote the NO release. However, even at a given temperature, it is still difficult to predict the NO flux at this stage because it is influenced by multiple factors including the water uptake of the bilayer coating, the NO donor amount and the hydrolysis rate of PLGA within the film. For example, the highest NO flux for the e-50-50-based film is observed on the second day even though the observed pH is higher on that day compared to the first day. This might be due to either the hydrolysis of e-50-50 that provides more protons that are quickly consumed by the NO donor or the increased water uptake of the film on the second day. Due to its fast hydrolysis rate, the gradually decreased daily NO flux observed for the a-50-50-based coating is most likely due to the continual depletion of the NO donor within the coating. The steady daily NO flux for the e-50-50-based coating, on the other hand, most likely results from the slower hydrolysis rate of the PLGA matrix that further yields a somewhat higher steady-state pH within the film.

The preliminary RT experimental results indicate that the hydrolysis rate of the specific PLGA used to formulate the films can be employed to control the release profile of the NO release coatings. At 37 °C, both the NO release rate of diazeniumdiolates and the hydrolysis rate of PLGA will be elevated. Since it is reported that a slower hydrolysis rate can be achieved by increasing the lactide ratio in the PLGA polymer chains [24], e-PLGAs with a lactide to glycolide ratio of 75:25 (e-75-25) and poly(lactic acid) (e-PLL) were also examined to prepare the NO release coatings for use at 37 °C. Fig. 4B shows the NO release profiles for four films containing 30 wt% DBHD/$N_2O_2$ doped into a-50-50, e-50-50, e-75-25

or e-PLL at 37 °C. The NO release profiles are consistent with the prediction from the RT results. The films are able to release NO for 3, 5, 8 and 10 d using the a-50-50, e-50-50, e-75-25 and e-PLL materials, respectively. The slower the PLGA hydrolysis rate, the longer the NO release persists. Due to the introduction of slower hydrolysis rate PLGAs, bromothymol blue (BB), with a higher transition pH range, was used to evaluate the film pH change for these four films at 37 °C. As shown in Fig. 5B, similar to the RT observations, the release of NO first increases the pH, and then further hydrolysis of PLGA provides additional protons to lower the film pH. From these comparisons, it is obvious that the hydrolysis rates of PLGAs are different within the coatings. For the a-50-50 (Fig. 5B-a) material, the hydrolysis of PLGA creates a very acidic environment already on the third day, and this contributes to the depletion of the NO donor. In contrast, the pH of the e-PLL film (Fig. 5B-d), is initially elevated due to the production of DBHD and remains almost neutral for 10 d due to the much slower hydrolysis of the PLL matrix [24]. For e-50-50 and e-75-25, the hydrolysis of PLGA causes an apparent color change indicating an acidic environment on the 5th (Fig. 5B-c) and 7th days (Fig. 5B-d), respectively.

The initial NO flux at a given temperature, however, is not related to the hydrolysis rate of the polymer, but the initial film pH. The acid capped PLGA, a-50-50, should be the matrix that creates the most acidic initial environment. For the ester-capped PLGAs, as listed in Supporting Information Table 1S, the monomer residue percentages are in the order of e-PLL > e-75-25 > e-50-50. Therefore, the initial pH of the films are in the order of a-50-50 < e-PLL < e-75-25 < e-50-50, which is further supported visually by comparing the film colors at 0 min (membrane pH a<d<c<b shown in Fig. 5B). The order of the initial NO flux of the four films, as shown in Fig. 4B (D1) and Supporting Information Fig. 3S-A, is consistent with the initial film acidity order, although the initial flux of the e-75-25-based film is only slightly higher than the film containing e-50-50-based film due to the small variation in their monomer residue percentages. Further, this data also suggests that it is possible to control the initial NO flux of the bilayer films by controlling the end groups and monomer residues within the PLGA polymer matrix used.

The NO release profile and the membrane pH of films containing other matrices such as SR and polyurethane (PU) instead of PLGA as the base layer were also studied and the results are shown in Supporting Information Fig. 3S. The difference between a PLGA matrix and SR or PU materials lies in the fact that the other two matrices lack the initial acid residues or the capability to hydrolyze to produce protons required for the NO donor to continuously produce NO. Therefore, when the control films with a base layer of 30 wt% DBHD/$N_2O_2$ doped in SR and PU are placed into PBS buffer at 37 °C, hardly any NO release is observed compared to films with the various PLGAs (Fig. 3S-A). A slight pH increase in the SR or PU-based films was observed over a one week period due to the production of DBHD, as shown in Fig. 3S-B. This confirms the important role of using PLGA as both an NO release promoter and controller in preparing the NO release coatings.

### 3.3 Antibiofilm properties of NO releasing bilayer films

Before the antibiofilm testing, an *in vitro* antimicrobial test was conducted to compare the influence of the NO releasing film and a series of control films on planktonic bacterial cells. The aim of the test was to study the “matrix” effect and further evaluate whether any leaching of trace amounts of the DBHD product was potentially toxic to the cells. An NO releasing film with 20 wt% DBHD/$N_2O_2$ mixed with a-50-50 PLGA as the inner layer was chosen because PLGA with the fastest hydrolysis rate is most likely to exhibit such problems. Therefore, two controls were used in this test, including a film with only PLGA (PLGA/SR) and a film with PLGA doped with 20 wt% diamine DBHD (20% DBHD) as the inner layer. In both cases, the SR top coating was present.

As shown in Fig. 6, when the NO releasing films and control films were placed into PBS buffer containing $10^8$ CFU/mL *S. aureus* (Fig. 6A) or *E. coli* (Fig. 6B) at 37 °C for 2 h, the NO releasing films showed ca. 1 log killing (i.e., the number of viable cells was reduced from ~$1.8\times10^8$ to ~$3.7\times10^7$ CFU/mL for *S. aureus* and ~$2.2\times10^8$ to ~$5\times10^7$ CFU/mL for *E. coli* ) compared to the controls that showed essentially no changes. After a 24 h exposure, with continuous release of NO as the antimicrobial agent, 3 logs of killing effect for both *S. aureus* and *E. coli* (i.e., the number of viable cells was reduced from ~$1.8\times10^8$ to ~$3.5\times10^5$ CFU/mL for *S. aureus* and for ~$2.2\times10^8$ to ~$3.1\times10^5$ CFU/mL for *E. coli* ) were observed. In contrast, a control film that contains only a SR top layer that exhibits almost no killing effect after 24 h exposure to bacterial suspension, the PLGA/SR or 20 wt% DBHD control films exhibit ca. 1 log killing effect for both bacterial strains, resulting from a “matrix” antimicrobial effect. However, this is much less than observed with the NO releasing coatings, confirming that NO is a potent antimicrobial agent for both gram-positive *S. aureus* and gram-negative *E. coli* [1]. If there is a significant leaching of the diamine DBHD, the 20 wt% DBHD control film should have exhibited a much greater killing effect compared to either the NO releasing film or the PLGA/SR control. However, since both controls exhibit almost identical effect on planktonic bacterial cells, only minimal leaching of DBHD from films with current configuration appears to occur. The minimal leaching of DBHD from the 20 wt% DBHD control film was also confirmed by mass spectrometry (see supporting information, Fig. 2S-C). When the same test was performed at RT (23 °C), none of the films exhibited any significant antimicrobial effect after 24 h (data not shown), indicating that higher temperature that leads to fast hydrolysis of the PLGA and increased release of NO also contributes to the observed “matrix” effect and antimicrobial effect of the NO releasing films.

Although the antibiofilm properties of NO releasing coatings have been demonstrated previously by both *in vitro* and *in vivo* studies [25, 26], there have been few examples that studied the influence of different NO release profiles on the antibiofim properties of the NO releasing coatings over a time scale that is long enough to form a mature biofilm. For example, the Schoenfisch group has evaluated and demonstrated the antibiofilm properties of NO releasing xerogel coatings against *S. aureus* in a subcutaneous animal model after implantation for 8 d [25]. However, considering that ca. 90% of the NO was released from their coatings over the initial 24 h period [25], it would be difficult to study the influence of the NO release profiles of this type of coating on the antibiofilm properties over an equivalent 8 d time-scale. Similarly, although *in vitro* studies under both stagnant and dynamic conditions have shown that NO releasing catheters are able to prevent biofilm formation by *E. coli*, the NO release profile of the catheter is not tunable and exhibits an initial “burst” of NO release [26]. Considering the complexity and time-scale of formation of a mature biofilm, the DBHD/$N_2O_2$-doped PLGA-based NO releasing coatings, with a tunable NO release profile over more than a week period, offers an ideal tool to study the influence of different NO release profiles on the degree of biofilm formation.

A CDC flow-through bioreactor was chosen to study the antibiofilm properties of the new NO release coatings because it is able to provide both shear forces and renewable nutrient sources that mimic an *in vivo* environment [13] and the test films are continuously exposed to the bacterial culture. This system has also been proven by statistical assessment to be a reliable tool for growing biofilms with repeatable results [27]. Compared to previously reported studies of microbial adhesion on NO releasing coatings in flowing systems for a short period of time with [26] or without [12, 14] nutrient sources, a seven-day biofilm test in a CDC bioreactor will better mimic a natural environment.

Therefore, the prepared NO releasing films and controls were first incubated in a CDC flow bioreactor at RT (23 °C) with gram-positive *S. aureus* or gram-negative *E. coli* cultures for 7

d. On the eighth day, the films were taken out of the reactor and stained with bacterial LIVE/DEAD dyes to visualize the growth of biofilm on different surfaces. The NO release profiles of the films are shown in Fig. 4 (see above), and Fig. 7 shows the representative fluorescent micrographs of the surfaces of NO releasing and control films after removal from the CDC bioreactor. As can be seen, for all the control films including PLGA/SR, 20 wt% DBHD and SR, the surfaces are fully colonized by mostly viable *S. aureus* or *E. coli* cells (shown as green dots). Both NO releasing films containing a base layer of 20 wt% DBHD/$N_2O_2$ doped in either a-50-50 or e-50-50 PLGA, exhibit clean surfaces. Compared to the a-50-50 PLGA-based NO releasing film that barely exhibits any observable bacterial cells on the surface, a small amount of bacterial cells are still observable on the e-50-50 PLGA-based film for both *S. aureus* and *E. coli*.. This might be attributable to the differences in the daily NO fluxes of the two films (see Fig. 4A), with the film with the higher NO flux exhibiting an enhanced antibiofilm effect. To better quantify the biofilm structure and biomass, 3D images were reconstructed based on the confocal images. The 3D images representing *S. aureus* biofilm formation on different surfaces at RT are shown in Fig. 8A and the quantitative analysis data are provided in Table 1. Similar to the fluorescent micrographs, the 3D images also confirm a significant antibiofilm effect of the NO releasing coatings. As shown in Fig. 8A, thick, dense and carpet-like biofilms containing mostly living *S. aureus* cells are developed on the surfaces of all the control films with some variations in the biofilm structures between the SR surface alone and the other two controls. The surfaces of the NO releasing films, on the other hand, have very few bacterial cells attached, indicating significant antibiofilm effect due to the NO release properties of the films. The biofilm biomass values quantified from the 3D images are listed in Table 1. Even for the e-50-50-based NO releasing film, a greater than 99.9% reduction of the biofilm biomass is obtained. Similar results were also obtained for *E. coli* (see Table 1). Interestingly, while neither of the NO releasing films exhibits observable antimicrobial effect in the antimicrobial test at RT, the antibiofilm properties are significant, even for the e-50-50 PLGA-based NO releasing film with a low NO flux. Viable cell counts before and after the antibiofilm test indicate that after one week growth in the medium, the bacterial concentration is ~100 times higher than the initial concentration (i.e., the viable cell counts increases from ~$1\times10^6$ CFU/mL to ~$2.7\times10^8$ CFU/mL for both *S. aureus* and *E. coli*). Due to the short lifetime of NO, it is impossible for it to diffuse far enough to kill all the planktonic bacterial cells in solution, especially if there is a limited amount of NO production. This might contribute to the lack of significant antimicrobial effects for the NO releasing films at RT using a suspension of living cells. However, since it is still possible for NO to interact with planktonic bacterial cells that are in close proximity to the coating surface, the NO releasing surface is able to create a localized “bacterial inhibition zone” as previously reported [26], that contributes to the observed antibiofilm effects observed on the surfaces. Further, it has been suggested that a low level of NO can induce the dispersal of diverse single- and multi-species biofilms of gram-positive and gram-negative bacteria through a signaling mechanism [2, 28]. Since the experimental results here indicate that the NO release coating with a relatively low daily NO flux (Fig. 4A, e-50-50) is also able to prevent biofilm formation, the observed antibiofilm effects of NO releasing coatings may also be derived from this dispersal mechanism. In addition, the dispersal of the biofilm will turn bacteria into planktonic state microbes, which will make the bacteria more susceptible to antimicrobial agents. Indeed, the observed antibiofilm effect of the NO releasing films can be considered to be the result of a synergic effect of both the antimicrobial and biofilm dispersal properties of NO. Further, to enhance the effectiveness of such films, conventional antibiotics could also be employed since they will have increased activity toward the dispersed biofilm microbes in the planktonic state, once the initial dispersal effects of NO occur.

The antibiofilm properties of NO releasing coatings with different NO release profiles (shown in Fig. 4B) were further evaluated at 37 °C and the representative fluorescent

micrographs of bacterial adhesion on different surfaces after the antibiofilm test are shown in Fig. 9. Compared to the SR surface that is fully colonized by bacterial cells after the antibiofilm test at RT (see Fig. 7), the biofilm formation on the same type of surface for either *S. aureus* or *E. coli* (Fig. 9) is less obvious at 37 °C. This is similar to the observations made by others, where *S. aureus* [29, 30] or *E. coli* [31] formed optimal biofilm at lower temperature, not at physiological conditions. Unlike the control SR surface, the control PLGA/SR and 30 wt% DBHD control film surfaces exhibit more dead cells compared to viable cells, indicating a "matrix" antimicrobial effect occurs at 37 °C. For both *S. aureus* and *E. coli*, the NO releasing surfaces are much less colonized compared to all the controls. This is consistent with the observations made in the solution-based antimicrobial testing at 37 °C, where NO releasing coatings exhibit much better killing effect on planktonic bacterial cells (Fig. 6). In addition, higher temperature might also increase the permeability of the cell membranes, which may also contribute to more dead or membrane damaged cells observed on the surfaces.

The antibiofilm effects of different NO releasing coatings, however, vary with bacterial strains and the NO release profiles. A difference was also observed in the viable cell counts after one week incubation at 37 °C for different bacterial strains in the CDC bioreactor. While the viable cell counts for *S. aureus* increased from ~1.8 $\times 10^6$ to ~ 8.6$\times 10^9$ CFU/mL, the growth of *E. coli* was slower (i.e., the viable cell counts increased from 1.6 $\times 10^6$ to 4.6 $\times 10^8$ CFU/mL). Therefore, the antibiofilm properties of the NO releasing films on different bacterial strains were compared separately. Firstly, for *S. aureus*, with a faster growth rate, although the formation of *S. aureus* biofilms on all the control films can clearly be observed (see Fig. 9), only a few dead or membrane damaged cells are observed on the surfaces of NO releasing films with different NO release profiles. The antibiofilm effects are almost identical for all the NO releasing films regardless of the differences in the lifetime of the films. However, the e-PLL-based NO releasing film, with the longest NO release lifetime (Fig. 4B), exhibits a cleaner surface. The 3D images for *S. aureus* biofilm formation on different surfaces are shown in Fig. 8B and the biomass values are quantified and listed in Table 2. Similar to the observations from the 2D images, the 3D images indicate that at RT, a denser and more evenly distributed *S. aureus* biofilm is formed on a SR surface compared to 37 °C. The calculated *S. aureus* biofilm biomass values for different surfaces listed in Table 2 further support the antibiofilm properties of the NO releasing coatings. With a biofilm biomass reduction of ca. 98.4% compared to the silicone rubber control, the e-PLL-based NO releasing coating that is able to release NO for the longest time period is the most effective coating to prevent *S. aureus* biofilm formation at 37 °C. The a-50-50, e-50-50 and e-75-25 PLGA-based coatings, all exhibit ca. 85% biofilm reduction despite variation in NO release lifetime of these coatings from 3 – 8 d. Compared to the e-75-25-based NO releasing coating, the better antibiofilm effect for the e-PLL-based coating might come from its higher NO flux on the eighth day when the film was removed from the CDC biofilm reactor.

When testing *E. coli*, the influence of different NO release profiles on the antibiofilm properties of the NO releasing films at 37 °C are more clearly observed. As shown in Fig. 9, for all the control films, a high percentage of the surface is colonized by *E. coli* cell clusters. Compared to the control SR surface where both viable and dead cells can be observed, most of the *E. coli* cells that are attached on either the PLGA or the 30 wt% DBHD control films are dead or membrane damages cells due to the "matrix" effect. Since the attachment of dead bacterial cells can trigger an immune response and inflammation [32], an "ideal" antibiofilm coating should be able to prevent the attachment of both living and dead bacterial cells [33]. Compared to the controls, the NO releasing coatings exhibit different degrees of antibiofilm behavior due to their different NO release profiles (Fig. 4B). It is obvious that the NO releasing coatings with a longer lifetime exhibit a cleaner surface (Fig. 9) and this effect is further supported by the *E. coli* biofilm biomass values listed in Table 2.

Indeed, the longer the NO release, the lower the *E. coli* biofilm biomass value. In particular, the e-PLL-based NO releasing coating is able to reduce the biofilm biomass by ca. 99.9%. However, for films prepared with all the other PLGA materials, > 99% biofilm reduction was also observed.

## 4. Conclusions

Nitric oxide releasing coatings with a bilayer configuration using DBHD/$N_2O_2$ doped within various PLGA materials were fabricated. By comparing the NO release profiles and film pH changes using PLGAs with different hydrolysis rates, it was shown that the specific chemical formulation of the PLGA used plays an important role as both a pH promoter and controller in the NO release mechanism. The new films with tunable NO releasing profiles were proven to prevent *S. aureus* and *E. coli* biofilm formation in a CDC flow bioreactor using a 7 d antibiofilm test. The proposed coatings are thus expected to be potentially useful as antibiofilm and antithrombotic coatings for preparation of indwelling devices (e.g., catheters) and future work will focus on further extending the NO release lifetimes of the coatings and conducting appropriate *in vivo* studies.

## Supplementary Material

Refer to Web version on PubMed Central for supplementary material.

## Acknowledgments

This work was supported by the National Institutes of Health (EB-004527 and EB-000783). The authors thank Dr. Kun Liu for her assistance with the DBHD/$N_2O_2$ synthesis, Dr. Hitesh Handa and Elizabeth Brisbois for providing the DBHD/$N_2O_2$ used in this study, Dr. Dipankar Koley and Elizabeth Brisbois for their helpful advice regarding the content and editing of this manuscript, and Elizabeth Brisbois for her help with the pH measurements of various THF solutions containing different species..

## References

[1]. Hetrick EM, Schoenfisch MH. Reducing implant-related infections: active release strategies. Chem Soc Rev. 2006; 35:780–9. [PubMed: 16936926]

[2]. McDougald D, Rice SA, Barraud N, Steinberg PD, Kjelleberg S. Should we stay or should we go: mechanisms and ecological consequences for biofilm dispersal. Nat Rev Micro. 2012; 10:39–50.

[3]. Campoccia D, Montanaro L, Speziale P, Arciola CR. Antibiotic-loaded biomaterials and the risks for the spread of antibiotic resistance following their prophylactic and therapeutic clinical use. Biomaterials. 2010; 31:6363–77. [PubMed: 20542556]

[4]. Busscher HJ, Ploeg RJ, van der Mei HC. SnapShot: Biofilms and biomaterials; mechanisms of medical device related infections. Biomaterials. 2009; 30:4247–8. [PubMed: 19618511]

[5]. Campoccia D, Montanaro L, Arciola CR. The significance of infection related to orthopedic devices and issues of antibiotic resistance. Biomaterials. 2006; 27:2331–9. [PubMed: 16364434]

[6]. Banerjee I, Pangule RC, Kane RS. Antifouling coatings: recent developments in the design of surfaces that prevent fouling by proteins, bacteria, and marine organisms. Adv Mater. 2011; 23:690–718. [PubMed: 20886559]

[7]. Stobie N, Duffy B, McCormack DE, Colreavy J, Hidalgo M, McHale P, et al. Prevention of Staphylococcus epidermidis biofilm formation using a low-temperature processed silver-doped phenyltriethoxysilane sol-gel coating. Biomaterials. 2008; 29:963–9. [PubMed: 18061256]

[8]. Stevens KNJ, Croes S, Boersma RS, Stobberingh EE, van der Marel C, van der Veen FH, et al. Hydrophilic surface coatings with embedded biocidal silver nanoparticles and sodium heparin for central venous catheters. Biomaterials. 2011; 32:1264–9. [PubMed: 21093906]

[9]. Barraud N, Hassett DJ, Hwang SH, Rice SA, Kjelleberg S, Webb JS. Involvement of nitric oxide in biofilm dispersal of Pseudomonas aeruginosa. J Bacteriol. 2006; 188:7344–53. [PubMed: 17050922]

[10]. Barraud N, Schleheck D, Klebensberger J, Webb JS, Hassett DJ, Rice SA, et al. Nitric Oxide Signaling in Pseudomonas aeruginosa Biofilms Mediates Phosphodiesterase Activity, Decreased Cyclic Di-GMP Levels, and Enhanced Dispersal. J Bacteriol. 2009; 191:7333–42. [PubMed: 19801410]

[11]. Partridge JD, Bodenmiller DM, Humphrys MS, Spiro S. NsrR targets in the Escherichia coli genome: new insights into DNA sequence requirements for binding and a role for NsrR in the regulation of motility. Mol Microbiol. 2009; 73:680–94. [PubMed: 19656291]

[12]. Hetrick EM, Schoenfisch MH. Antibacterial nitric oxide-releasing xerogels: Cell viability and parallel plate flow cell adhesion studies. Biomaterials. 2007; 28:1948–56. [PubMed: 17240444]

[13]. Williams DL, Bloebaum RD. Observing the biofilm matrix of Staphylococcus epidermidis ATCC 35984 grown using the CDC biofilm reactor. Microsc Microanal. 2010; 16:143–52. [PubMed: 20205969]

[14]. Privett BJ, Nutz ST, Schoenfisch MH. Efficacy of surface-generated nitric oxide against Candida albicans adhesion and biofilm formation. Biofouling. 2010; 26:973–83. [PubMed: 21082455]

[15]. Frost MC, Reynolds MM, Meyerhoff ME. Polymers incorporating nitric oxide releasing/generating substances for improved biocompatibility of blood-contactincy medical devices. Biomaterials. 2005; 26:1685–93. [PubMed: 15576142]

[16]. Batchelor MM, Reoma SL, Fleser PS, Nuthakki VK, Callahan RE, Shanley CJ, et al. More lipophilic dialkyldiamine-based diazeniumdiolates: Synthesis, characterization, and application in preparing thromboresistant nitric oxide release polymeric coatings. J Med Chem. 2003; 46:5153–61. [PubMed: 14613318]

[17]. Yan QY, Major TC, Bartlett RH, Meyerhoff ME. Intravascular glucose/lactate sensors prepared with nitric oxide releasing poly(lactide-co-glycolide)-based coatings for enhanced biocompatibility. Biosens Bioelectron. 2011; 26:4276–82. [PubMed: 21592764]

[18]. Qin Y, Bakker E. Quantitive bindin constants of H+ -selective chromoionophores and anion ionophores in solvent polymeric sensing membranes. Talanta. 2002; 58:909–18. [PubMed: 18968823]

[19]. Castegnaro M, Massey RC, Walters CL. The collaborative evaluation of a procedure for the determination of N-nitroso compounds as a group. Food Addit Contam. 1987; 4:37–43. [PubMed: 3556674]

[20]. Heydorn A, Nielsen AT, Hentzer M, Sternberg C, Givskov M, Ersboll BK, et al. Quantification of biofilm structures by the novel computer program COMSTAT. Microbiology. 2000; 146:2395–407. [PubMed: 11021916]

[21]. Davies KM, Wink DA, Saavedra JE, Keefer LK. Chemistry of the diazeniumdiolates. 2. Kinetics and mechanism of dissociation to nitric oxide in aqueous solution. J Am Chem Soc. 2001; 123:5473–81. [PubMed: 11389629]

[22]. Ding AG, Schwendeman SP. Acidic Microclimate pH Distribution in PLGA Microspheres Monitored by Confocal Laser Scanning Microscopy. Pharm Res. 2008; 25:2041–52. [PubMed: 18622692]

[23]. Li L, Li SM, Sun JH, Zhou LL, Bao XG, Zhang HG, et al. Diversity enhances agricultural productivity via rhizosphere phosphorus facilitation on phosphorus-deficient soils. Proc Natl Acad Sci U S A. 2007; 104:11192–6. [PubMed: 17592130]

[24]. Li SM. Hydrolytic degradation characteristics of aliphatic polyesters derived from lactic and glycolic acids. J Biomed Mater Res. 1999; 48:342–53. [PubMed: 10398040]

[25]. Nablo BJ, Prichard HL, Butler RD, Klitzman B, Schoenfisch MH. Inhibition of implant-associated infections via nitric oxide. Biomaterials. 2005; 26:6984–90. [PubMed: 15978663]

[26]. Regev-Shoshani G, Ko M, Miller C, Av-Gay Y. Slow release of Nitric Oxide from Charged Catheters and Its Effect on Biofilm Formation by Escherichia coli. Antimicrob Agents Chemother. 2010; 54:273–9. [PubMed: 19884372]

[27]. Goeres DM, Loetterle LR, Hamilton MA, Murga R, Kirby DW, Donlan RM. Statistical assessment of a laboratory method for growing biofilms. Microbiology-Sgm. 2005; 151:757–62.

[28]. Barraud N, Storey MV, Moore ZP, Webb JS, Rice SA, Kjelleberg S. Nitric oxide-mediated dispersal in single- and multi-species biofilms of clinically and industrially relevant microorganisms. Microb Biotechnol. 2009; 2:370–8. [PubMed: 21261931]

[29]. Williams DL, Woodbury KL, Haymond BS, Parker AE, Bloebaum RD. A Modified CDC biofilm reactor to produce mature biofilms on the surface of PEEK membranes for an in vivo animal model application. Curr Microbiol. 2011; 62:1657–63. [PubMed: 21437591]

[30]. Rode TM, Langsrud S, Holck A, Moretro T. Different patterns of biofilm formation in Staphylococcus aureus under food-related stress conditions. Int J Food Microbiol. 2007; 116:372–83. [PubMed: 17408792]

[31]. Andersen TE, Kingshott P, Palarasah Y, Benter M, Alei M, Kolmos HJ. A flow chamber assay for quantitative evaluation of bacterial surface colonization used to investigate the influence of temperature and surface hydrophilicity on the biofilm forming capacity of uropathogenic Escherichia coli. J Microbiol Methods. 2010; 81:135–40. [PubMed: 20188127]

[32]. Cheng G, Xite H, Zhang Z, Chen SF, Jiang SY. A switchable biocompatible polymer surface with self-sterilizing and nonfouling capabilities. Angew Chem Int Ed. 2008; 47:8831–4.

[33]. Webb JS, Thompson LS, James S, Charlton T, Tolker-Nielsen T, Koch B, et al. Cell death in Pseudomonas aeruginosa biofilm development. J Bacteriol. 2003; 185:4585–92. [PubMed: 12867469]

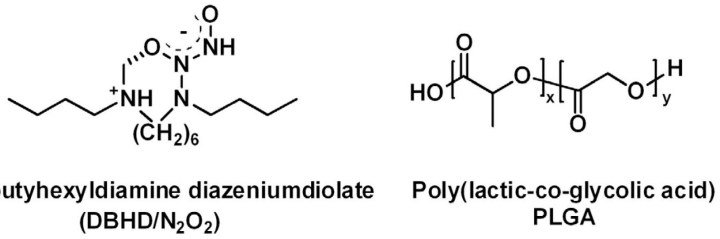


**Fig. 1.**
Structures of dibutyhexyldiamine diazeniumdiolate (DBHD/$N_2O_2$) and poly(lactic-*co*-glycolic) acid (PLGA).

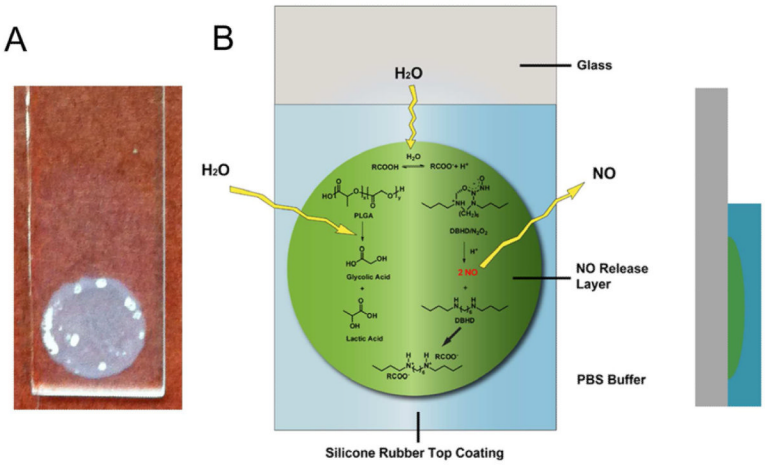


**Fig. 2.**

A) the appearance of dibutyhexyldiamine diazeniumdiolate (DBHD/$N_2O_2$) and poly(lactic-*co*-glycolic) acid (PLGA)-based NO releasing coating with a bi-layer structure on a glass slide B) Schematic illustration of dibutyhexyldiamine diazeniumdiolate (DBHD/$N_2O_2$) and poly(lactic-*co*-glycolic) acid (PLGA)-based NO releasing coating and its cross-section.

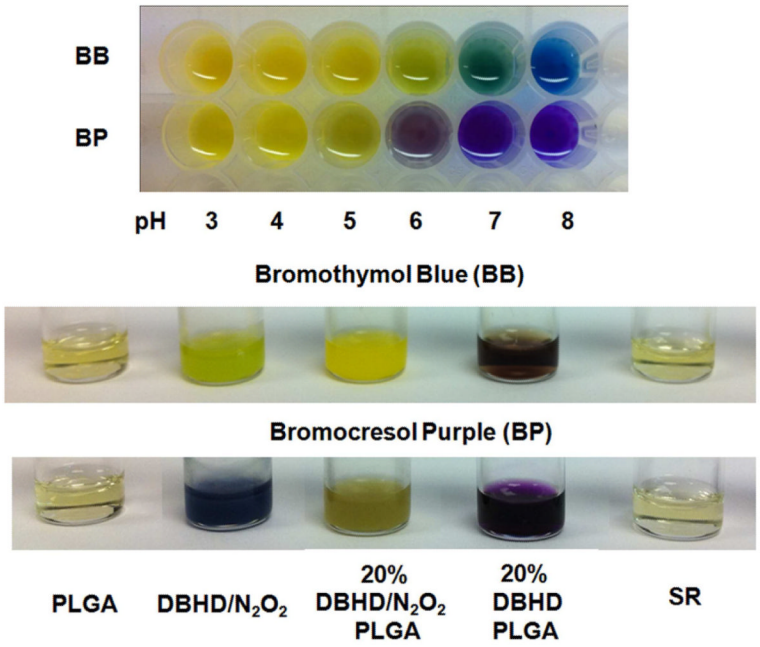


**Fig. 3.**

Comparison of color changes of bromothymol blue (BB) and bromocresol purple (BP) in different solutions or cocktails including pure PLGA, DBHD/$N_2O_2$, 20 wt% DBHD/$N_2O_2$ mixed in PLGA, 20 wt% DBHD in PLGA and silicone rubber THF solution (The concentration for all polymer solution is 200mg/3mL). a-50:50 lactide: glycolide PLGA is used for all the experiment. The indicator concentration is 10 mmol $kg^{-1}$. The colors of the solutions were compared rightly after the solutions were prepared. The color chart below indicates the variation of indicator colors with pH in PBS buffer.

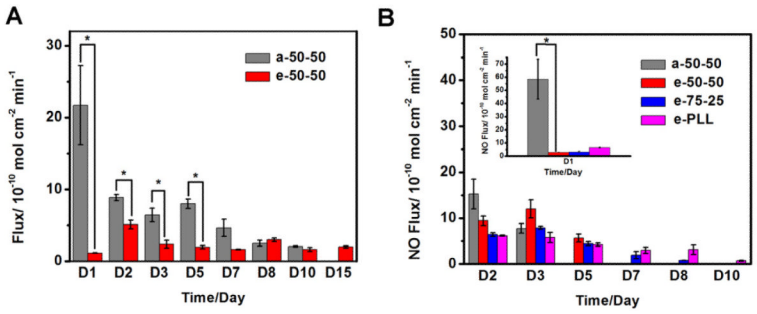


**Fig. 4.**

NO release profiles of NO releasing films with a base layer containing 20 wt% DBHD/$N_2O_2$ in a-50-50 and or e-50-50 at RT (A) and 30 wt% DBHD/$N_2O_2$ in a-50-50, e-50-50, e-75-25 or e-PLL at 37 °C (B). The NO flux was recorded on a chemiluminescence NO analyzer (NOA). The fluxes presented are the average of two films (n=2). *, $P<0.05$ (the fluxes of a-50-50-based NO releasing films are significantly different from the fluxes of e-50-50-based films).

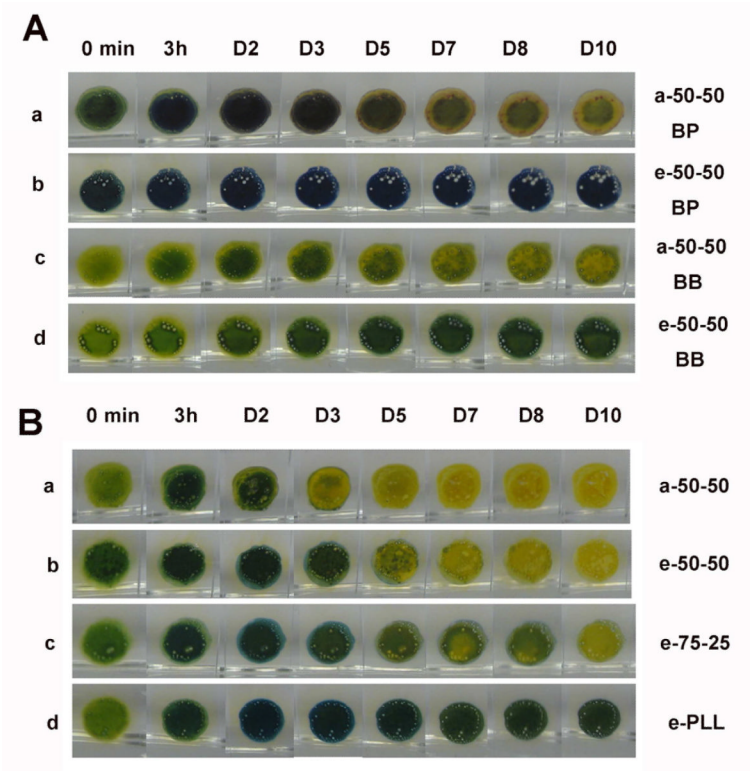


**Fig. 5.**

A) comparison of color changes of bromothymol blue (BB) or bromocresol purple (BP) doped NO releasing films containing a base layer of 20 wt% DBHD/$N_2O_2$ in a-50-50 and or e-50-50 at RT B) comparison of color changes of bromothymol blue (BB) doped NO releasing films containing a base layer of 30 wt% DBHD/$N_2O_2$ in a-50-50, e-50-50, e-75-25 or e-PLL at 37 °C for 10d.

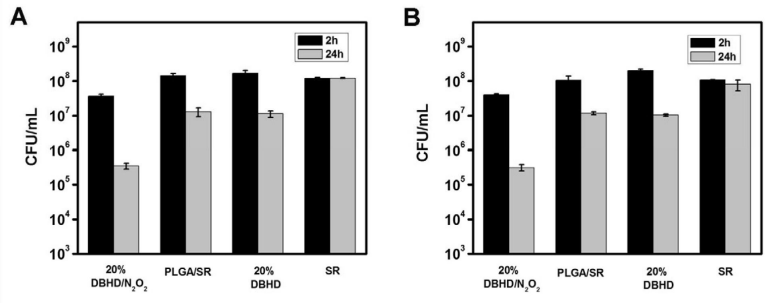


**Fig. 6.**

The killing effects of NO releasing films with a base layer of 20 wt% DBHD/$N_2O_2$ doped in a-50-50, control films with a base layer of a-50-50, 20 wt% DBHD doped in a-50-50 and control film with only SR top coating on (A) *S. aureus* and (B) *E. coli* after 2 h and 24 h incubation at 37 °C in $10^8$ CFU/mL bacterial suspension.

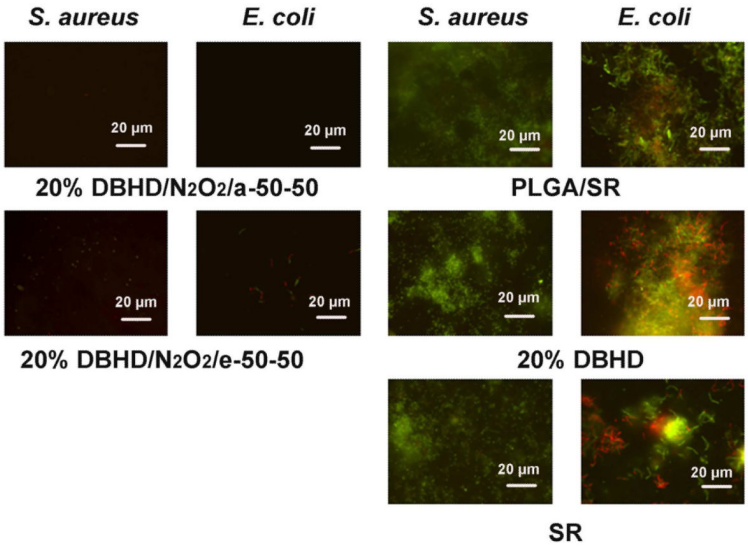


**Fig. 7.**

Representative fluorescent micrographs showing comparison of surfaces of NO releasing and control films after incubation at RT (23 °C) for seven days in a CDC biofilm reactor containing *S. aureus* or *E. coli*. The NO releasing films containing a base layer of 20 wt% DBHD/$N_2O_2$ mixed with a-50-50 or e-50-50 PLGA matrix, and the NO release profile of the films are shown in Fig. 4A. The controls include two films with base layers of a-50-50 PLGA or a-50-50 PLGA mixed with 20 wt% DBHD and a film with only a SR layer. Bacterial cells were stained with Bacterial LIVE/DEAD staining dyes and viable cells shown as green fluorescent dots while dead or membrane damaged cells shown as red fluorescence dots in the images.

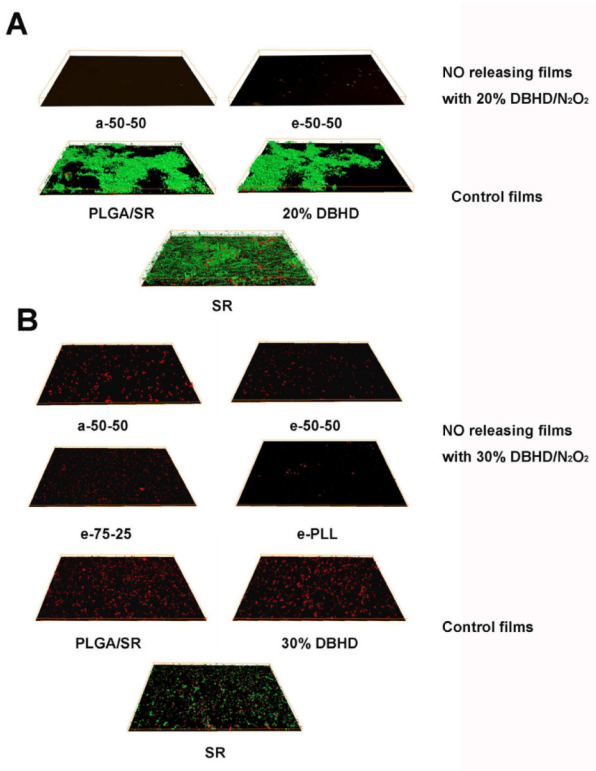


**Fig. 8.**

Three-dimensional images of *S. aureus* biofilm formed (A) at RT on NO releasing films with a base layer of 20 wt% DBHD/$N_2O_2$ doped in a-50-50 or e-50-50 PLGA and control films with a base layer of a-50-50, a-50-50 mixed with 20 wt% DBHD or a control film with only a silicone rubber top coating. The dimension of the films are 142 × 108 × 15 μm (B) at 37 °C on NO releasing film with a base lay er of a) 30 wt% DBHD/$N_2O_2$ doped in a-50-50, e-50-50, e-75-25 or e-PLL PLGA matrix and control film with a base layer of a-50-50, a-50-50 mixed with 30 wt% DBHD and a film with only a silicone rubber top coating after incubation in a CDC biofilm reactor after seven days. The dimension of the films are 142 × 108 × 9 μm. Bacterial cells were stained with Bacterial LIVE/DEAD staining dyes and viable cells shown as green fluorescent dots while dead or membrane damaged cells shown as red fluorescence dots in the images.

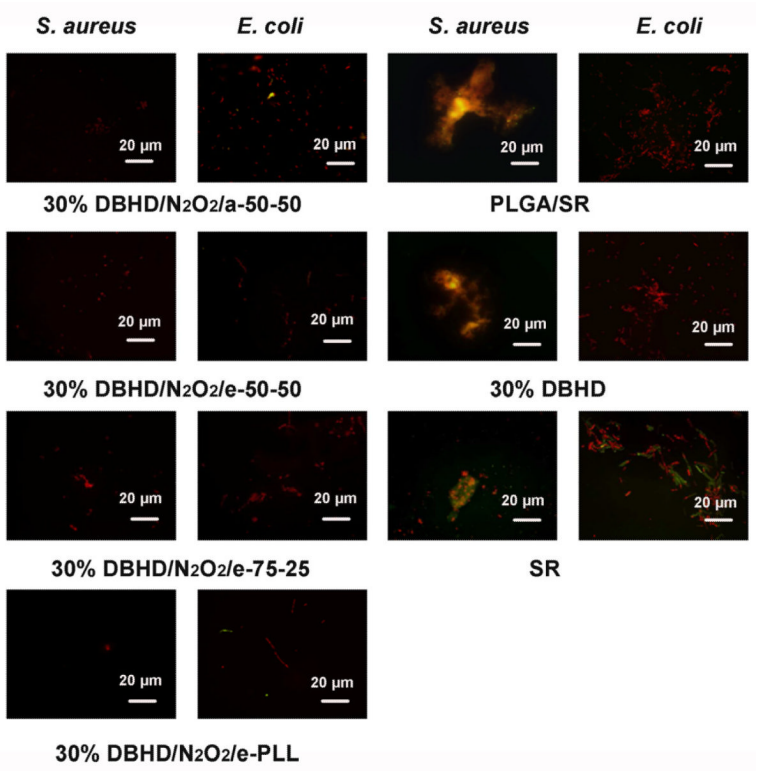


**Fig. 9.**

Representative fluorescent micrographs showing comparison of surfaces of NO releasing and control films after incubation for seven days at 37 °C in a CDC biofilm reactor containing *S. aureus* or *E. coli*. The NO releasing films containing a base layer of 30 wt% DBHD/$N_2O_2$ mixed with a-50-50, e-50-50, e-75-25 or e-PLL PLGA matrix, and the NO release profile of the films are shown in Fig. 4B. The controls include two films with base layers of a-50-50 PLGA or a-50-50 PLGA mixed with 30 wt% DBHD and a film with only a SR layer. Bacterial cells were stained with Bacterial LIVE/DEAD staining dyes and viable cells shown as green fluorescent dots while dead or membrane damaged cells shown as red fluorescence dots in the images.

## Table 1

Biofilm biomass in *S. aureus* and *E. coli* biofilm on PLGA-based bilayer films in CDC biofilm reactor at RT.[a]

| Films | | *S. aureus* Biomass/$\mu m^3/\mu m^2$ | *E. coli* Biomass/$\mu m^3/\mu m^2$ |
|---|---|---|---|
| NO release | a–50–50 | 0 (±0) | 0 (±0) |
| | e–50–50 | 1.5 (±0.3)×$10^{-3}$ | 1.8 (±0.8)×$10^{-3}$ |
| Control | PLGA/SR | 5.2 (±0.7) | 4.9 (±0.5) |
| | 20% DBHD | 4.1 (±0.6) | 5.7 (±2.4) |
| | SR | 3.6 (±0.4) | 4.4 (±0.6) |

[a]Average values with standard deviations for n= 2 shown in the brackets were calculated from COMSTAT image analysis on CLSM images.

## Table 2

Biofilm biomass in *S. aureus* and *E. coli* biofilm on PLGA- or PLL-based bilayer films in CDC bioreactor at 37 °C.[a]

| Films | | *S. aureus* Biomass/$\mu m^3/\mu m^2$ | *E. coli* Biomass/$\mu m^3/\mu m^2$ |
|---|---|---|---|
| NO release | a–50–50 | $8.6\ (\pm 1.0)\times 10^{-3}$ | $4.0\ (\pm 1.2)\times 10^{-3}$ |
| | e–50–50 | $8.3\ (\pm 3.6)\times 10^{-3}$ | $1.3\ (\pm 0.5)\times 10^{-3}$ |
| | e–75–25 | $9.2\ (\pm 7.5)\times 10^{-3}$ | $7.0\ (\pm 4.8)\times 10^{-4}$ |
| | e–PLL | $9.4\ (\pm 6.0)\times 10^{-4}$ | $1.6\ (\pm 0.6)\times 10^{-4}$ |
| Control | PLGA/SR | $1.4\ (\pm 1.6)\times 10^{-2}$ | $4.0\ (\pm 1.8)\times 10^{-1}$ |
| | 30% DBHD | $5.9\ (\pm 2.5)\times 10^{-2}$ | $4.0\ (\pm 1.0)\times 10^{-1}$ |
| | SR | $5.9\ (\pm 0.5)\times 10^{-2}$ | $6.0\ (\pm 1.4)\times 10^{-1}$ |

[a]Average values with the standard deviations for n = 2 shown in the brackets were calculated from COMSTAT image analysis on CLSM images.